

Dynamics of Viral RNA Synthesis during Measles Virus Infection

Sébastien Plumet,¹ W. Paul Duprex,² and Denis Gerlier^{1*}

Immunité & Infections Virales, CNRS-University of Lyon 1 UMR 5537, IFR Laennec, 69372 Lyon Cedex 08, France,¹ and School of Biology and Biochemistry, The Queen's University of Belfast, 97 Lisburn Road, Belfast, Northern Ireland BT9 7BL, United Kingdom²

Received 20 October 2004/Accepted 19 January 2005

We propose a reference model of the kinetics of a viral RNA-dependent RNA polymerase (vRdRp) activities and its regulation during infection of eucaryotic cells. After measles virus infects a cell, mRNAs from all genes immediately start to accumulate linearly over the first 5 to 6 h and then exponentially until ~24 h. The change from a linear to an exponential accumulation correlates with de novo synthesis of vRdRp from the incoming template. Expression of the virus nucleoprotein (N) prior to infection shifts the balance in favor of replication. Conversely, inhibition of protein synthesis by cycloheximide favors the latter. The in vivo elongation speed of the viral polymerase is ~3 nucleotides/s. A similar profile with fivefold-slower kinetics can be obtained using a recombinant virus expressing a structurally altered polymerase. Finally, virions contain only encapsidated genomic, antigenomic, and 5'-end abortive replication fragment RNAs.

Viruses are obligate intracellular parasites. To understand the complexity of virus replication and to develop potent antiviral drugs, there is a growing need for a systematic analysis of the underlying molecular mechanisms. Although the kinetics of protein expression has been established for many viruses and a model of the dynamics of virus transcription and replication for bacteriophage Q has been proposed (see reference 10 for a review), knowledge in this area is very limited for all eucaryotic viruses. We report the first kinetics model of the transcription and replication of a negative-sense, single-stranded RNA virus.

Measles virus (MV) belongs to the order *Mononegavirales* (33). The replication strategy involves a viral RNA-dependent RNA polymerase (vRdRp), which uses as a template a nucleocapsid (NC) made of a single strand of RNA in tight complex with the nucleoprotein (N). The negative-strand genome contains six transcription units encoding the N, phospho (P), matrix (M), fusion (F), hemagglutinin (H), and large (L) or polymerase protein, in that order (Fig. 1). The transcription units are flanked by short leader (Le) and trailer (Tr) sequences containing the genomic promoter (on the minus strand) and the antigenomic promoter (on the plus strand), respectively. The P gene also encodes the nonstructural V and C proteins by RNA editing and alternative overlapping open reading frame, respectively.

Every N protein binds to 6 nucleotides so that the N polymer entirely covers the 15,894-nucleotide genome (5) and makes it resistant to nucleases (33). NC comprises 2,649 N, ~300 P, and ~20 to 50 L proteins (33) and is enclosed within a membrane envelope containing H and F glycoproteins. After fusion with the plasma membrane at neutral pH, intact NCs are released into the cytoplasm (24), where they serve as a template for both primary transcription from and replication of the genomic RNA (Fig. 1). Transcription is initiated from a single promoter

at the 3' end of the genome (for a review, see reference 23) by vRdRp made of L and P proteins. Immediately prior to an intergenic junction, the transcriptase recognises a gene end signal and terminates the synthesis of the upstream mRNA. Then, it either recognizes the gene start (GS) signal of the downstream gene and begins the synthesis of mRNA or fails to do so and detaches from the template. As a consequence, there is an attenuated gradient of viral transcription (7). Sometimes, the transcriptase fails to recognize the intergenic junction, and read-through leads to the generation of bicistronic mRNAs (7). Following an ill-defined signal, the vRdRp switches to a replicative mode and uses the upstream replication genomic promoter to synthesize a full-length positive-sense RNA strand. Concomitant encapsidation during RNA elongation probably explains the rarity of viral recombination events observed within the order *Mononegavirales* (38) and makes the RNA resistant to small interfering RNA (RNA interference silencing) (4, 35). NC likely associates with cellular (co)factors, which contribute to the overall vRdRp functionality (15).

The homo-oligomeric P protein acts as a bridge between L and the NC template (8). P protein also binds newly synthesized, monomeric forms of the 60-kDa N protein (N^o) to form a soluble (N^o-P) complex (22). The N^o-P complex is thought to be the substrate used by the vRdRp to initiate the encapsidation of the nascent RNA chain during replication (14, 22).

Study of the functions and regulations of the vRdRp has been hampered so far by the lack of a convenient in vitro acellular or cellular RdRp assay and by our very poor knowledge of the kinetics of the vRdRp during virus infection. By using reverse transcription-quantitative PCR (RT-QPCR), we reliably quantify MV RNA species and describe the kinetics of their accumulation during the infection.

MATERIALS AND METHODS

Cell culture and viruses. Human HeLa and 293T cells were grown as previously described (9). MV Hallé or Edmonston strain and recombinant MV EdtagL-MMEGFPM expressing a chimeric fluorescent L polymerase containing enhanced green fluorescent protein (EGFP) (9) were maintained in Vero cells. Cell-free virus was purified from the supernatant of Vero-infected cells by sed-

* Corresponding author. Mailing address: Immunité & Infections Virales, CNRS-University of Lyon 1 UMR 5537, IFR Laennec, 69372 Lyon Cedex 08, France. Phone: 33 (0)4 78 77 86 18. Fax: 33 (0)4 78 77 87 54. E-mail: Denis.Gerlier@univ-lyon1.fr.

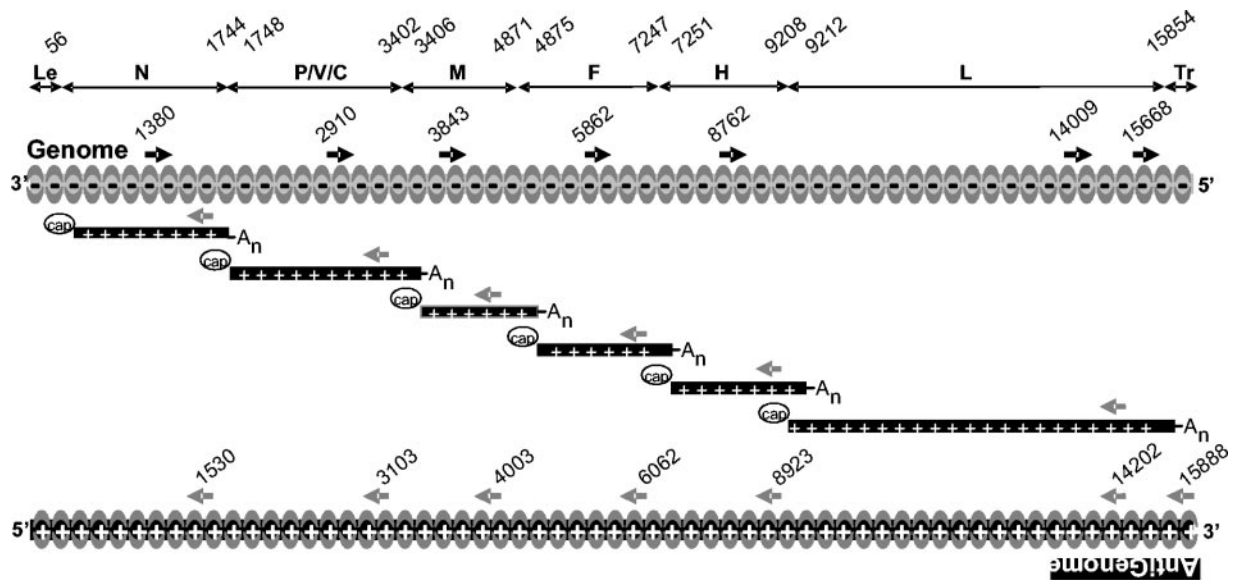


FIG. 1. Schematic view of MV genomic organization, main RNA species, and nucleotide positions of gene starts and gene ends indicated above the 15,894-nucleotide-long genome. Sense and antisense primers with their first nucleotide positions are indicated by black and grey arrows, respectively. Antisense primers above mRNAs and above antigenome are identical.

imentation on a discontinuous sucrose gradient as detailed previously (26). Infections at a multiplicity of infection (MOI) of 1 were performed at 37°C for 2 h in the absence of serum. Alternatively, MV infection was synchronized by allowing virus binding to the cells for 30 min at 4°C.

RNA preparation and reverse transcription. Total RNA was extracted from cells lysed with either the RNeasy kit (QIAGEN) or TRIZol reagent (Invitrogen). To isolate RNA protected by N protein, infected cells were lysed for 1 h at 37°C in the presence of 0.1 U of micrococcal nuclease (Sigma) diluted in 20 mM Tris, 50 mM NaCl, 1 mM CaCl₂, 1% (vol/vol) NP-40, and 0.1 mM 1,10-phenanthroline, 0.1 mM 3,4-dichloroisocoumarin, and 0.02 mM E-64 as protease inhibitors. Then, RNA was extracted. The quantity and purity of RNA were checked by measuring absorbance at 260 nm and 280 nm and by verifying the integrity of rRNA of every sample by agarose gel electrophoresis and ethidium bromide labeling (Euromedex).

For specific RT, 0.2 µg of total RNA was reverse transcribed with 10 pmol of primers, 10 nmol of deoxynucleoside triphosphates, 2 µl of 10× RT buffer (Stratagene), and 25 U of Stratascript enzyme (Stratagene) in a final volume of 20 µl for 50 min at 48°C after an initial denaturing step at 70°C for 5 min in the absence of the enzyme. For random and oligo(dT) RT, 2 µg of total RNA was reverse transcribed with 0.4 µg of random hexamer primers (Promega) and 0.4 µg of oligo(dT) 15 (Promega), 25 nmol of deoxynucleoside triphosphates, 2 µl of RT 10× buffer, and 25 U of Stratascript enzyme in a final volume of 20 µl for 90 min at 48°C after the initial denaturing step. cDNA/RNA complexes from the RT were diluted 10 fold in nuclease-free water before PCR. RT efficiency was linear over a 100-fold concentration as ascertained by PCR (data not shown).

Quantitative PCR. Primers were designed using LC Probe Design (Roche) and Primer3 software (http://www.broad.mit.edu/cgi-bin/primer/primer3_www.cgi). The localization of MV primers is indicated in Fig. 1. Cellular housekeeping ribosomal 18S and actin RNA was also quantified with specific primers. QPCR was performed using FastStart DNA Master SYBR Green I reagents and with the Light Cycler apparatus from Roche Diagnostic (Meylan, France). Reactions were performed with 1.5 µl of enzyme mixture from the kit, 10 pmol of sense primers, 10 pmol of antisense primers, and 5 µl of diluted RT product in a final volume of 20 µl. Every PCR was performed as follows: initial denaturation at 95°C for 10 min and 45 amplification cycles, including annealing, elongation, fluorescence measurement, and denaturation steps. At the end of the PCR, melting temperature of the final double-strand DNA product was determined with intercalated SYBR Green. Special care was taken to achieve amplification efficiencies closest to 2 (i.e., synthesis of only full-length DNA amplicons at each cycle) and to measure only specific amplicons. This was facilitated by the selection of optimal primer and MgCl₂ concentrations and running conditions for each pair of primers and by the addition of a heating step prior to measurement

of fluorescence to avoid the fluorescence from nonspecific primer dimers. Settings were considered acceptable when PCR efficiency was >1.85, when the error type between standard points and regression curve was <0.1, and when amplification generated a single amplicon of the expected size (150 to 200 bp) that exhibited a single, sharp fusion curve. Amplicons were quantified by plotting the values against standard curves made using 10-fold dilutions of plasmids encoding either individual MV genes and/or a plasmid (pMV2A) that contains a cDNA copy of the complete viral genome (30). Data were expressed as copy numbers either per cell or per 2 µg of RNA. In some experiments, the total number of polymerized nucleotides (corresponding to total mRNAs, genomes, and antigenomes) accumulated over a time period was calculated by assuming a constant elongation speed and by taking into account the transcription attenuation according to the values determined in this work. All experiments were carried out at least twice with similar results.

Immunolabelling and flow cytometry. HeLa or 293T cells (10⁶) were transfected with pSC6-N, pSC6-N-his, pSC6-N-myc, pSC6-P, and pSC6-M plasmids (each, 5 µg) encoding, respectively, N, N with a six-His epitope tag at the C terminus, N with a *c-myc* epitope tag at the C terminus, P proteins, and M proteins using Lipofectamine (Invitrogen) (30; S. Plumet and D. Gerlier, unpublished data). pBluescript was transfected in all negative controls. Cells were cotransfected at a ratio of 1/3 with pCDNA3-MCAM-gfp encoding cell surface hybrid avian MCAM-gfp (1) as a positive marker of transfection. Twenty-four hours posttransfection, cells were infected by MV Hallé strain at an MOI of 1. At 24 h postinfection (hpi), MV membrane proteins were labeled using BMS94 simian serum anti-MV (43) and detected with an anti-human phycoerythrin conjugate. For flow cytometry analysis, only cells which expressed EGFP were analyzed for the expression of MV proteins. Sorting of infected and noninfected cells was performed according to the level of expression of viral antigens (with the cutoff values of the fluorescence background set to include >99.5% of the noninfected cells).

Data analysis. The kinetics of RNA accumulation was analyzed using Excel software (Microsoft) by plotting best-fitting regression curves. The doubling time (*dt*) was calculated from the regression curve equations $n = a \times \exp^{bt}$, where *n* is the number of RNA copies and *t* is time, according to the formula: $dt = \ln(2)/b$.

RESULTS

Relative quantification of individual MV segments from a genomic RNA template. RNA, purified from micrococcal nuclease treated MV-infected HeLa cell lysates, was reverse tran-

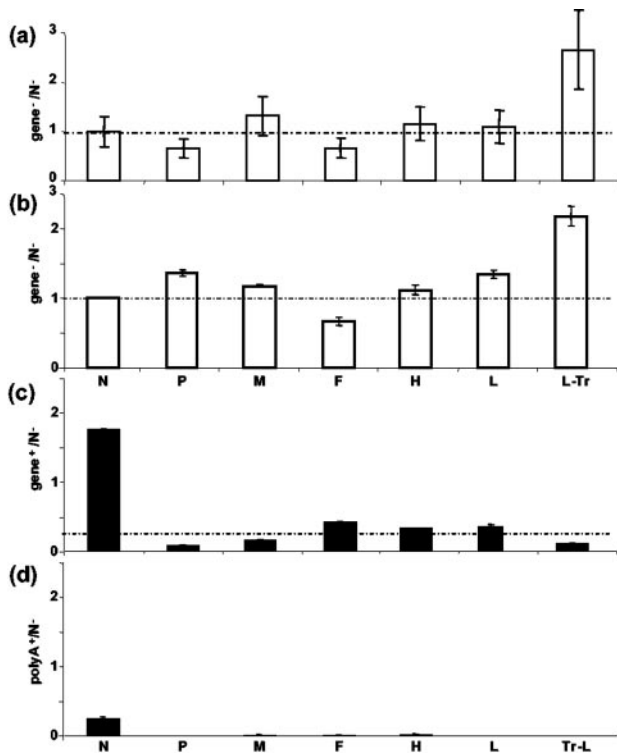


FIG. 2. Relative quantification of individual MV segments (as ratios of gene to N negative-strand RNA) from a genomic RNA template (a) and purified virions after RT (b to d) with mixed sense (a and b), mixed antisense (c), and oligo(dT) (d) primers. Equimolar ratios are indicated by dotted lines. The genomic template was prepared from MV-infected cell lysate treated with micrococcal nuclease before RNA extraction and reverse transcription with a mixture of specific positive-sense primers.

scribed using a mixture of specific positive-sense primers, and cDNAs were quantified by QPCR. As expected from a unique negative-stranded RNA template, equimolar ratios of individual MV gene segments were found, with MVgene/N gene ratios comprising between 0.7 ± 0.2 and 1.3 ± 0.3 , except for a 2.6-fold excess of the L-Tr segment, which corresponds to the genome species (Fig. 2a). A difference in the PCR step was excluded because equimolar ratios were obtained from QPCR analysis of a plasmid encoding a full-length antigenome of Moraten MV strain (a kind gift of R. Cattaneo) (data not shown). Thus, the excess in L-Tr amplicons reflects either a difference at the RT step or an excess of encapsidated abortive genome.

RNA content of measles virions. After RT of negative-stranded RNAs from purified Edmonston MV particles with a mixture of sense primers, equimolar ratios of individual MV cDNA segments were obtained, except for a 2.2-fold excess of L-Tr amplicons (Fig. 2b). These data mirror those obtained from genomic RNA extracted from infected cells (Fig. 2a). After RT of positive-stranded RNAs (antigenome and mRNAs) using antisense primers, equimolar ratios were also observed except for a ~ 5 -fold excess of the 5'-end N amplicon (Fig. 2c). Each positive-stranded RNA (except N) was about $\sim 20\%$ of its negative-stranded counterpart (compare Fig. 2c with Fig. 2b). Only a few copies of poly(A) N mRNA were

detected, amounting to $\sim 20\%$ of the positive-stranded N RNA after RT with an oligo(dT) primer (Fig. 2d). Similar data were obtained after RT of RNA purified from solubilized MV particles pretreated with micrococcal nuclease, independently of the use of a sense, antisense, or oligo(dT) primer (data not shown). Overall, these data indicate that only encapsidated RNAs are incorporated into the viral particles. They corresponded to full-length genome and antigenome in approximately a 5-to-1 ratio and to excess 5'-end sequences of both the genome L-Tr and the antigenome N sequence, which may also have included the 5' leader sequence, so we called them (Le-) N, one-fifth of them being polyadenylated. Since only a 5'-end excess was detected, we excluded a PCR artifact.

Assessment of the transcription gradient in infected cells. The availability of validated primer sets led us to quantify the amount of mRNAs for each viral gene during the course of an infection. Until now, the only means to examine this was by using Northern blot technology which is less sensitive, time consuming, and not well suited for simultaneous analysis of numerous samples. HeLa cells were infected at an MOI of 1, and total RNA was isolated at 48 hpi. The RNA was reverse transcribed with random hexamers and oligo(dT), L-Tr-positive, or negative-sense primers, and cDNAs were quantified. Since positive-stranded RNA represents both RNA transcripts and antigenome, the number of antigenome copies was subtracted from the number obtained for each mRNA transcript (single-gene RNA copies) to evaluate RNA transcripts. A 3'-to-5' transcription gradient was observed with $31,300 \pm 10,000$ N, $4,800 \pm 1,500$ P, $4,960 \pm 400$ M, $4,400 \pm 1,300$ F, $3,560 \pm 160$ H, 540 ± 150 L, $1,030 \pm 190$ genome, and 130 ± 20 antigenome RNA copies/cell. These figures compared well with those previously reported after Northern blot analysis of MV-infected Vero cells (7). Although our quantification assay could not distinguish between monocistronic and polycistronic mRNA, the contributions of bicistronic mRNAs which can account for up to 30% of the messages (7) were within (or close to) the error range of our assay.

Kinetics of MV RNA accumulation. After a synchronized infection, N mRNA accumulated without any detectable lag phase between 0 and 8 h (Fig. 3a), where the amount detected at $t = 0$ represented the RNA input. P, M, F, H, and L RNAs accumulated at a rate similar to that of N, starting from a similar amount representing about one-fifth that of the initial N RNA amount but accumulating with decreasing rates according to the expected transcription gradient (not shown). Between 2 and 24 hpi, N RNA accumulated at an apparent exponential rate (Fig. 3b) before reaching a plateau, followed by a slow decrease between 24 and 48 hpi. The accumulation of P, M, F, H, and L RNAs followed similar kinetics at decreasing rates. Thus, the transcription gradient was maintained throughout the infection. The kinetics of genome and antigenome accumulation was strikingly different. The levels of genome and antigenome did not vary by more than twofold until 10 to 12 hpi (Fig. 3c), and then they accumulated exponentially until 48 hpi (Fig. 3b) but at a lower rate between 24 and 48 hpi.

After infection by EdtagL-MMEGFPM at an equivalent MOI N, F, and genomic RNAs accumulated at a much slower rate (Fig. 4a). However, without any detectable lag time, N and F mRNA accumulated in parallel linearly over the first 8 h then exponentially (Fig. 4b). The genome copy number remained

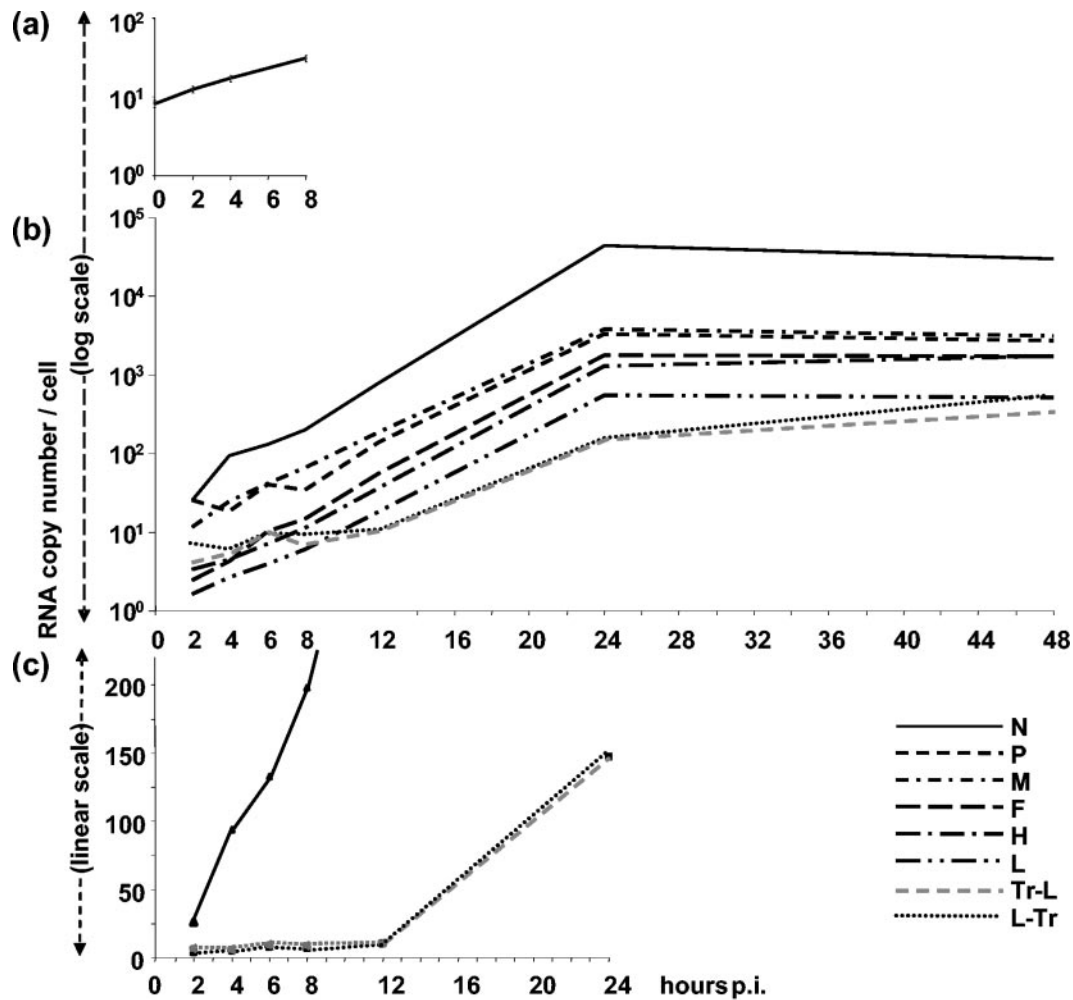


FIG. 3. Kinetics of accumulated mRNAs, genome, and antigenome after RT of total RNA from Hallé virus-infected cells with random and oligo(dT), sense, and antisense primers, respectively. (a) N RNA accumulation. (b and c) MV gene, genome, and antigenome accumulation every 2 h from 2 to 12, 24, and 48 hpi plotted in semilogarithmic (b) and linear (c) scales. Standard deviations ($\pm 15\%$) are not shown for clarity. Data collected at intermediate time points between 12 to 24 and 24 to 48 hpi during other experiments also fit with the drawn curves.

constant up to 8 hpi, and then it started to accumulate, reaching exponential growth after 24 hpi. Thus, when compared to the Hallé strain, EdtagL-MMEGFP started to replicate after a similar delay but at a much slower rate.

Incoming viral polymerases are stable over 6 h. In the first 12 h of infection, i.e., before any significant replication occurred which would increase the number of viral templates, the kinetics of N mRNA accumulation was linear for the first 5 h, after which time the curve changed abruptly to an exponential phase (Fig. 5a). We hypothesized that this sudden change in N mRNA levels may reflect the activity of newly synthesized vRdRps. In the presence of cycloheximide, the general inhibitor of protein synthesis, the RNA accumulation curve was indistinguishable from that observed in nontreated cells for the first 5 h (Fig. 5a). However, after 5 to 6 hpi, the two curves abruptly diverged; in the presence of cycloheximide, the accumulation rate did not switch to exponential phase. N mRNA accumulation remained the same for ~ 1 h, after which time the levels declined to the starting value by 12 hpi, indicating that either viral transcription was extinguished and/or N

mRNA was degraded at an increasing rate. However, the level of genomic RNA remained stable and was not affected by cycloheximide. A generalized activation of cellular ribonucleases induced by cycloheximide was excluded because the amounts of cellular actin mRNA and ribosomal 18S RNA remained constant over the 12-h cycloheximide treatment (not shown). Thus, the activity of newly synthesized vRdRps became detectable 5 hpi, and incoming vRdRp were active for at least 6 h.

Balance of RNA synthesis switching from replication to transcription. Adding cycloheximide at 16 hpi resulted in a complete arrest in replication, since the number of genomic RNA copies at 22 hpi was identical to that observed at 16 hpi (Fig. 5b). However, the accumulated P mRNA levels increased compared to the untreated sample. When cycloheximide treatment started at 24 hpi, the overall data were very similar, with replication inhibited and transcription increased. The total amount of RNA synthesis was not significantly changed when protein synthesis was inhibited (Fig. 5c). Furthermore, in the absence of cycloheximide, transcription slowed down at later

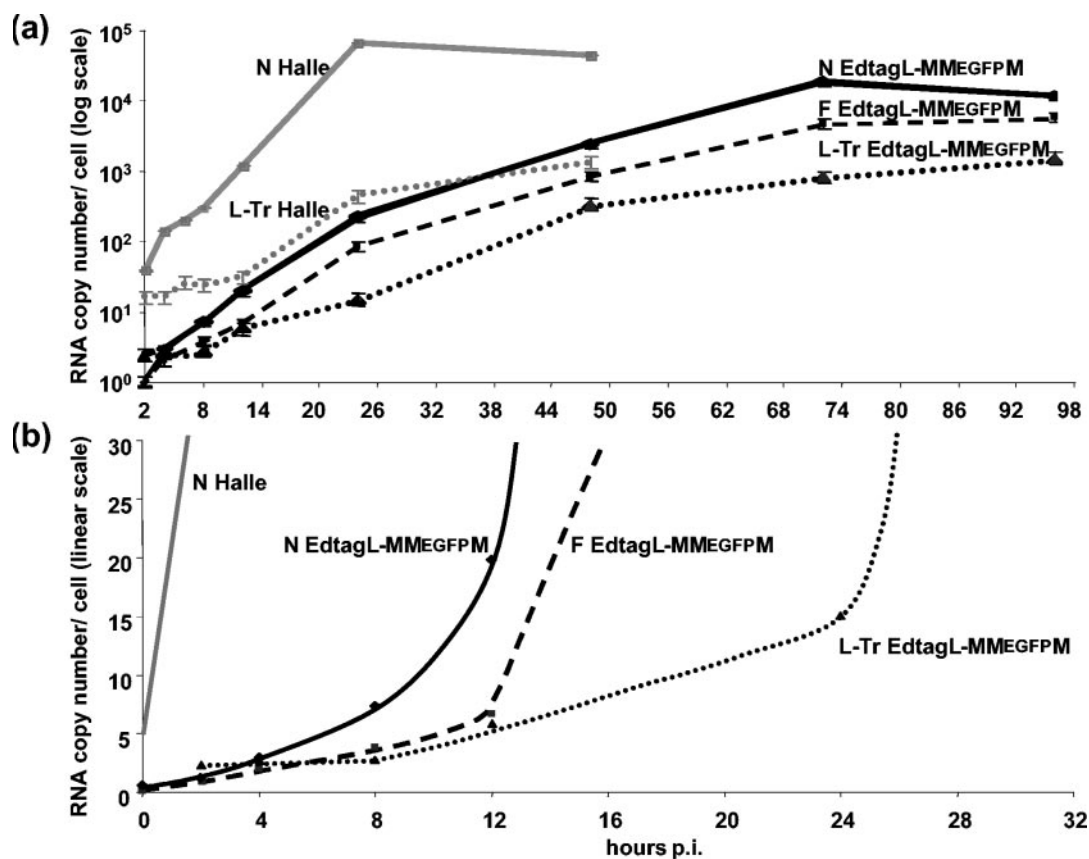


FIG. 4. Kinetics of N (solid line), F (dashed line), and genome (dotted line) RNA accumulation in EdtagL-MMEGFPM virus-infected cells after RT of total RNA with random and oligo(dT) (N and F), and sense (genome) primers, plotted in semilogarithmic (a) or linear (b) scale. N RNA and genome accumulation during infection by MV Hallé strain is shown by grey lines. Standard deviations ($\pm 15\%$) are not shown for clarity.

times, since there was a 2.0-fold and 1.4-fold increase of the P mRNA copies from 16 to 22 hpi and from 24 to 30 hpi, respectively. In contrast, the replication level remained constant with a 4.5-fold and 4.4-fold increases of genome RNA copies from 16 to 22 hpi and 24 to 30 hpi, respectively.

Stimulation of viral replication by overexpressing MV N protein before infection. From the above data, newly synthesized viral proteins are generated from 5 hpi, a time when active nascent vRdRps could be detected. However, this was not immediately followed by replication. The delay before the onset of replication suggested that N may need to accumulate above a threshold concentration to permit a switch to replication. When N protein was expressed by transient transfection for 24 h before the MV infection, the H mRNA-to-genome ratio at 24 hpi was reduced from 5.9 ± 1.40 to 1.17 ± 0.10 (Fig. 6a). However, the numbers of nucleotides polymerized were comparable, $\sim 6.3 \cdot 10^{10}$ and $\sim 4.9 \cdot 10^{10}$ per 2 μ g of total RNA, respectively. Thus, overexpression of N favors the switch from transcription to replication. As a result, one should expect an overall decrease in MV protein expression when N is expressed prior to MV infection. Indeed, when virus-infected 293T cells overexpressed different versions of N (N wild type, six-His-tagged N, or N-myc) prior to infection, the number of cells expressing a detectable amount of H and F glycoproteins at the cell surface decreased from $\sim 75\%$ to $\sim 40\%$, $\sim 31\%$, and $\sim 38\%$, respectively. In contrast, the transient expression of

MV P or MV M protein had little or no effect on the replication/transcription ratio, due to the increased N protein concentration at an early time after infection.

DISCUSSION

We used a validated and optimized RT-QPCR to analyze the RNA contents of measles virions and to obtain a dynamic view of the viral RNA accumulation during the course of infection. The assay was reliable for absolute quantification of the RNA synthesized from individual MV genes, genomes, and antigenomes with a standard deviation not exceeding $\pm 20\%$ for the overall process. All data were reproducible (compare Fig. 2a and 2b, 3c and 5a; data not shown).

Encapsulation is a necessary and sufficient signal for RNA packaging into virus. Compared to other members of the *Paramyxoviridae* (33), MV buds rather poorly and tends to remain cell associated. Furthermore, virions are pleiomorphic (42). However, NC packaging and virus budding are selective processes, excluding nonencapsidated viral mRNAs, which are in a 30-fold excess over that of the genomes and antigenomes in infected cells. We suggest that genomes and antigenomes share the same packaging signal because they are found in a similar ratio in virions and infected cells.

In addition, we found a two- and fivefold molecular excess of encapsidated 5'-end minus-strand Tr-L and plus-strand Le-N

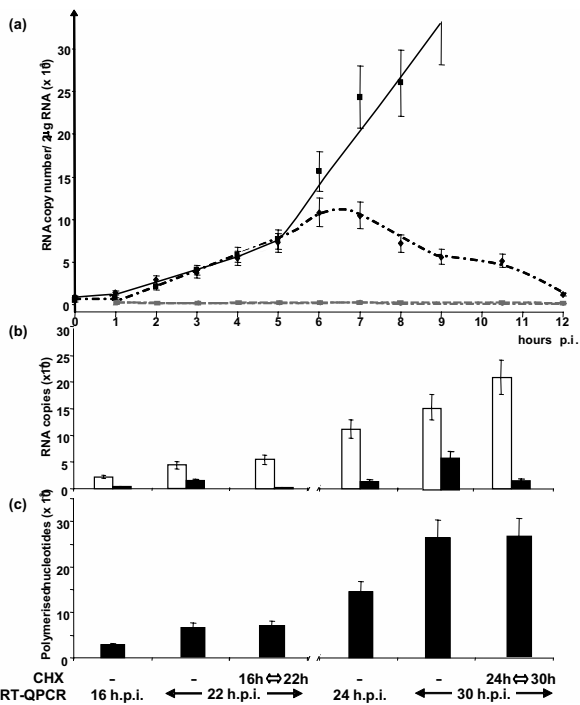


FIG. 5. (a) Kinetics of N mRNA (black symbols and lines) and genome (grey symbols and line) accumulation in the absence (solid line and squares) or presence (dotted lines, diamonds, and triangles) of 20 μg/ml cycloheximide. (b and c) Effect of cycloheximide on transcription and replication activities. (b) Levels of accumulated P mRNAs (white columns) and genome (black columns) measured at the times indicated. (c) Total RNA synthesis (black columns) calculated from the data shown above.

sequences, respectively, the latter being partly poly(A) and having been reported previously (6). They can result from either abortive replications and/or a switch failure between transcription and replication. The poly(A) species (reference 6 and this report) could be made by a replicase incorrectly recognizing the polyadenylation site at the end of the N gene. Interestingly, the lack of simultaneous excess of both 3' and 5' ends indicates a lack of contamination of our viral stocks with internal-deletion defective interfering particles. In summary, encapsidation appears as a both necessary and sufficient signal to induce specific packaging of NC into budding virions.

A model of MV RNA accumulation kinetics during infection.

From mathematical analyses of our data, we built a model describing MV RNA accumulation kinetics after infection which comprises five discrete phases (Fig. 7). Since MV mRNAs (27) and encapsidated antigenomic RNA (Fig. 5a) are stable at least over 6 h, RNA accumulation should accurately reflect the viral RNA synthesis.

In the first phase lasting from 0 to ~5 hpi, incoming vRdRps initiated primary transcription from every gene with no detectable lag phase. Every mRNA accumulated linearly, indicating a constant number of active transcriptases. Active transcriptases bound to the incoming template are also detected in the case of rabies virus, another member of the *Mononegavirales* (37). By assuming a constant number of templates uninterruptedly transcribed during the first 5 h into N mRNA, we could estimate an elongation speed of three nucleotides/s, meaning

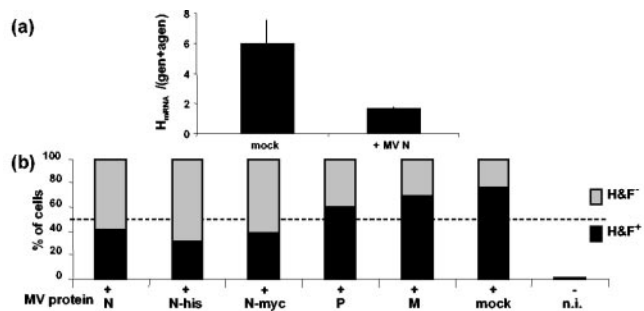


FIG. 6. Stimulation of viral replication by overexpression of MV N protein before infection. (a) H mRNA and genome plus antigenome ratio accumulated at 24 hpi in cells expressing N or not 24 h prior to infection. The amount of H mRNA was calculated after deduction from the genome and antigenome contribution and that of genome plus antigenome was calculated after deduction from the abortive 5'-end L-Tr and (Le-)N sequences with the ratios calculated from the data shown in Fig. 2 and 3. Total RNA was reverse transcribed with random and oligo(dT) primers to avoid any difference from the RT step. (b) The percentage of cells expressing H and F glycoproteins after the expression of MV N, His-tagged N, N-myc, P, or M 24 h prior to infection.

that a 2-kb-long mRNA would be transcribed in less than 12 min. This is in good agreement with elongation rates determined in vitro for Sendai virus (1.7 nucleotides/s) (11) and vesicular stomatitis virus (VSV) (3.1 to 4.3 nucleotides/s) (2) RdRp, but this rate is about 100-fold slower than that of the T7 polymerase (25). Several peculiarities may contribute to the slower RNA elongation speed of *Mononegavirales* vRdRps. (i) The RNA template has its phosphate backbone covered by an N protein every 6 nucleotides (18); during RNA elongation, it is expected to dissociate temporarily from N (23). (ii) vRdRp progression relies on the cartwheeling of tetrameric P proteins along the NC through the dynamic interaction of their C-terminal X domains with the N_{TAILS} (24). (iii) The vRdRp caps and polyadenylates the mRNAs. Assuming that vRdRp generates messenger, genomic, and antigenome RNAs at the same speed, as observed for Sendai virus and VSV (2), the MV RdRp would require at least ~1.5 h to replicate the 15,894 nucleotide genome or antigenome and ~2 h if we take into account the 2- to 5-min delay necessary to cross a gene junction, as determined for VSV (19).

Including the EGFP moiety within L protein (9) slows the vRdRp elongation speed down to 0.6 nucleotides/s. Therefore, when commencing from the 3'-end transcription promoter, the slow-elongating vRdRp of EdtagL-MMEGFPM should only complete the first F and L mRNA in less than ~3.3 h and ~7.2 h, respectively (Fig. 1). The lack of such a lag phase indicates that some vRdRps must already be close to the F (and every other) gene start just before virus entry. Thus, the incoming NC template should be associated with several vRdRps; this is in agreement with the observed distribution of P and L proteins on NCs extracted from Sendai virions (28). Furthermore, inside virus particles, the vRdRps seem to be kept in a "ready-to-go" state. The lack of detectable active new transcriptases before 8 h in the case of EdtagL-MMEGFPM MV indicates that the incoming ones can survive and be active at least over 8 h after virus entry.

In the second phase, lasting from ~5 to ~12 h, mRNA accumulates exponentially. Being transcribed from a constant

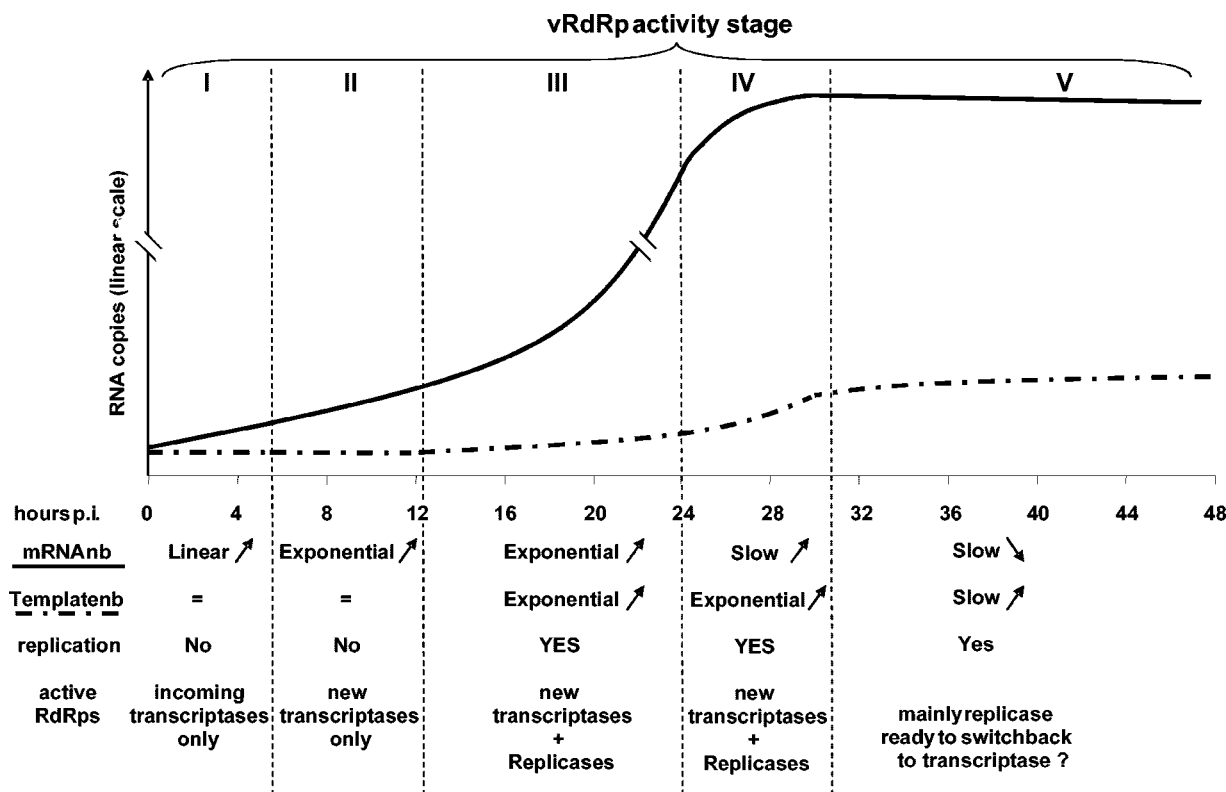


FIG. 7. Model of RdRp activities during MV infection. During the first 5 to 6 h of infection, only viral mRNAs synthesized by RdRp brought by the virions accumulated linearly (phase I). Between 5 to 6 and 10 to 12 hpi, viral mRNAs accumulated exponentially because of the additional transcriptase activities of newly synthesized RdRps (phase II). Between 10 to 12 and ~24 hpi, some RdRp switched to replicase activity, leading to exponential accumulation of genomes and antigenomes (phase III). Between ~24 and ~30 hpi, viral transcripts accumulation slowed down (phase IV). In the last phase V, less and less RdRps had transcriptase activity, whereas replication somehow slowed down.

number of genome templates, new transcriptases are recruited. Indeed, the inhibition of newly synthesized vRdRps keeps the mRNA accumulation constant, at least over the first 6 to 7 h. The first-order kinetics of the exponential mRNA accumulation indicates a regular increase in the number of transcriptases. As a result, vRdRps should accumulate on the NC template, in agreement with the observation of additional P binding sites on Sendai virus NCs (36) and enriched areas in P and L proteins observed on cytoplasmic active Sendai virus NCs (28). Since the longest gene (L) is completed in less than 40 min, the 5- to 6-h delay in the appearance of newly synthesized RdRps likely reflects the time for protein synthesis and/or the need for newly synthesized L-P complexes to reach a concentration threshold before being recruited.

From the parallel accumulation kinetics of the six transcripts, the transcription attenuation at each gene junction is estimated as ~77% between N and P, ~20% between P and M, ~69% between P and M, ~44% between F and H, and ~47% between H and L, in agreement with a previous report (7). Interestingly, EdtagL-MMEGFPM virus displays equivalent levels of transcriptional attenuation. This transcriptional attenuation differs from that of VSV (2) and from that of Sendai virus (13; C. Giorgi and D. Kolakofsky, personal communication). Since the genome is transcribed in ~1.5 to 2 h, the linear accumulation of all mRNA over 5 to 6 h by a fixed number of incoming vRdRps implies that the majority must

efficiently reattach to the NC. When arriving at an intergenic junction, the vRdRp scans to the next transcription start site (23) and either transcribes the next gene or detaches from the template (24). How vRdRps, which dissociate from the template at an intergenic junction, so efficiently find their way back to the single transcriptional promoter in the 3'-end Le remains an area of speculation. We propose that vRdRps, which fail to reinitiate, may continue to travel towards the genome end through P cartwheeling on N_{TAILS} instead of detaching (23). They could then jump to a leader localized nearby. The leader-to-trailer proximity could be the result of a circular arrangement of full-length genome NCs, which have sometimes been observed in electron microscopy (3, 40), or of the head-to-tail arrangement of two genomes, since MV can be naturally diploid or polyploid (31).

During the third phase, from ~12 to ~24 hpi, mRNAs, genomes, and antigenomes accumulate exponentially because of the increase of both newly available template and vRdRp. Surprisingly, the exponential increase of the templates is not associated with a boost in the mRNA accumulation, if only a few of them are effectively transcribed as previously suggested (34). During the fourth phase, from ~24 to ~30 hpi, genomes and antigenomes continue to accumulate exponentially at the same rate, whereas the accumulation of the transcripts slows down. In the last phase, genome and antigenome accumulation slows down, and the cell content in viral transcripts tends to

decrease. The progressive loss of vRdRp activities during the last two phases may reflect either the high virus release, which decreases the overall intracellular concentration at this stage, and/or the progressive cell damage induced by MV infection.

Is the switch between transcription and replication bidirectional? *Mononegavirales* vRdRps functioning as replicases have features distinct from those acting as transcriptases. Replication consists of the synthesis of (anti)genome RNA and its simultaneous encapsidation by N monomers provided as N^o-P complexes. These activities are coupled, and the replication of Sendai virus genome in vitro requires the N protein (24). VSV replicase and transcriptase complexes differ by the presence of the N protein (29). As observed for *Rhabdoviridae* (2), N expression promotes MV replication, and its concentration seems to constitute an important component of the switch to replication. It also induces a decrease in transcription, suggesting that polymerases involved in replication are diverted from their ongoing transcriptase activity. It is still unknown if transcription and replication can occur simultaneously on a single genomic NC. Conversely, as reported for all *Mononegavirales* studied so far (see reference 24 for a review), the inhibition of protein synthesis blocks MV replication (12). Correlatively, there is an increase in transcription, which suggests that vRdRps initially committed to replication may have reverted to transcription. An increase in transcription induced by cycloheximide has been reported at 3 days postinfection (20) but not at 16 hpi (12). The latter result could result from the use of an assay not sensitive enough to detect the small additional effect of the switch from replication to transcription (Fig. 7). Thus, any vRdRp previously committed to replication would be reused as a transcriptase. This would explain how any virion-associated vRdRp could act as a transcriptase.

The pool of soluble N protein available as a soluble N^o-P complex (17, 22–24, 39) for the encapsidation of nascent genome or antigenome quickly becomes limiting upon arrest of protein synthesis, even later in the infection when large amounts of N protein accumulate in intracellular inclusions. In the case of Sendai virus, nearly all newly synthesized P and L associate with NCs within few minutes. Conversely, only 30% of N does so, and the remaining part exists as a soluble pool, half of which is retrieved in 3.5 h and become progressively associated with NC (21). In the case of VSV, the existing pool of N, P, and L proteins can sustain replication only for about 20 min after arrest of protein synthesis (35). We postulate that the N^o-P complex has a very short half-life; consequently, replication likely requires a continuous flow of newly synthesized complex.

In conclusion, from the first kinetic assessment of viral RNA accumulation during infection by a member of the *Mononegavirales*, a testable model of the dynamics between transcriptase and replicase has been built, allowing the study of different virus to host cell combinations such as infection of lymphocytes or dendritic cells by wild-type isolates. Furthermore, this model could help to unravel the role of the nonstructural C and V proteins in transcription and/or replication (16, 32, 41), the mechanism leading to the nonpermissiveness of some cells (44), the antiviral effect of interferon, and the regulation of the vRdRp activities in persistently infected cells of neural origin.

ACKNOWLEDGMENTS

We thank D. Kolakofsky, L. Roux, F. Iseni, and S. Longhi for helpful comments and discussions.

S.P. is supported by the Délégation Générale pour l'Armement. This work was supported in part by the Medical Research Council (grant ID 63468) and the Commission of the European Communities, specifically, the RTD program "Quality of Life and Management of Living Resources," QLK2-CT2001-01225.

This work does not necessarily reflect the views of the Commission of the European Communities and in no way anticipates the Commission's future policy in this area.

REFERENCES

- Alais, S., N. Allili, C. Pujades, J. L. Duband, O. Vainio, B. A. Imhof, and D. Dunon. 2001. HEMCAM/CD146 downregulates cell surface expression of beta1 integrins. *J. Cell Sci.* **114**:1847–1859.
- Barr, J. N., S. P. Whelan, and G. W. Wertz. 2002. Transcriptional control of the RNA-dependent RNA polymerase of vesicular stomatitis virus. *Biochim. Biophys. Acta* **1577**:337–353.
- Bhella, D., A. Ralph, and R. P. Yeo. 2004. Conformational flexibility in recombinant measles virus nucleocapsids visualised by cryo-negative stain electron microscopy and real-space helical reconstruction. *J. Mol. Biol.* **340**:319–331.
- Bitko, V., and S. Barik. 2001. Phenotypic silencing of cytoplasmic genes using sequence-specific double-stranded short interfering RNA and its application in the reverse genetics of wild type negative-strand RNA viruses. *BMC Microbiol.* **1**:34.
- Calain, P., and L. Roux. 1993. The rule of six, a basic feature for efficient replication of Sendai virus defective interfering RNA. *J. Virol.* **67**:4822–4830.
- Castaneda, S. J., and T. C. Wong. 1989. Measles virus synthesizes both leaderless and leader-containing polyadenylated RNAs in vivo. *J. Virol.* **63**:2977–2986.
- Cattaneo, R., G. Rebmann, A. Schmid, K. Baczkó, V. ter Meulen, and M. A. Billeter. 1987. Altered transcription of a defective measles virus genome derived from a diseased human brain. *EMBO J.* **6**:681–688.
- Curran, J. 1996. Reexamination of the Sendai virus P protein domains required for RNA synthesis: a possible supplemental role for the P protein. *Virology* **221**:130–140.
- Duprex, W. P., F. M. Collins, and B. K. Rima. 2002. Modulating the function of the measles virus RNA-dependent RNA polymerase by insertion of green fluorescent protein into the open reading frame. *J. Virol.* **76**:7322–7328.
- Eigen, M. 2002. Error catastrophe and antiviral strategy. *Proc. Natl. Acad. Sci. USA* **99**:13374–13376.
- Gubbay, O., J. Curran, and D. Kolakofsky. 2001. Sendai virus genome synthesis and assembly are coupled: a possible mechanism to promote viral RNA polymerase processivity. *J. Gen. Virol.* **82**:2895–2903.
- Hall, W. W., D. Genius, and V. ter Meulen. 1977. The effect of cycloheximide on the replication of measles virus. *J. Gen. Virol.* **35**:579–582.
- Homann, H. E., P. H. Hofschneider, and W. J. Neubert. 1990. Sendai virus gene expression in lytically and persistently infected cells. *Virology* **177**:131–140.
- Horikami, S. M., J. Curran, D. Kolakofsky, and S. A. Moyer. 1992. Complexes of Sendai virus NP-P and P-L proteins are required for defective interfering particle genome replication in vitro. *J. Virol.* **66**:4901–4908.
- Horikami, S. M., and S. A. Moyer. 1995. Structure, transcription, and replication of measles virus. *Curr. Top. Microbiol. Immunol.* **191**:35–50.
- Horikami, S. M., S. Smallwood, and S. A. Moyer. 1996. The Sendai virus V protein interacts with the NP protein to regulate viral genome RNA replication. *Virology* **222**:383–390.
- Huber, M., R. Cattaneo, P. Spielhofer, C. Orvell, E. Norrby, M. Messerli, J. C. Perriard, and M. A. Billeter. 1991. Measles virus phosphoprotein retains the nucleocapsid protein in the cytoplasm. *Virology* **185**:299–308.
- Iseni, F., F. Baudin, D. Garcin, J. B. Marq, R. W. Ruigrok, and D. Kolakofsky. 2002. Chemical modification of nucleotide bases and mRNA editing depend on hexamer or nucleoprotein phase in Sendai virus nucleocapsids. *RNA* **8**:1056–1067.
- Iverson, L. E., and J. K. Rose. 1981. Localized attenuation and discontinuous synthesis during vesicular stomatitis virus transcription. *Cell* **23**:477–484.
- Kiley, M. P., and F. E. Payne. 1974. Replication of measles virus: continued synthesis of nucleocapsid RNA and increased synthesis of mRNA in the presence of cycloheximide. *J. Virol.* **14**:758–764.
- Kingsbury, D. W., C. H. Hsu, and K. G. Murti. 1978. Intracellular metabolism of Sendai virus nucleocapsids. *Virology* **91**:86–94.
- Kolakofsky, D., and B. M. Blumberg. 1982. A model for the control of non-segmented negative strand virus genome replication, p. 203–213. *In* B. W. J. Mahy, A. C. Minson, and G. K. Darby (ed.), *Virus persistence*. Cambridge University Press, Cambridge, United Kingdom.
- Kolakofsky, D., P. Le Mercier, F. Iseni, and D. Garcin. 2004. Viral RNA polymerase scanning and the gymnastics of Sendai virus RNA synthesis. *Virology* **318**:463–473.

24. Lamb, R. A., and D. Kolakofsky. 2001. *Paramyxoviridae*: the viruses and their replication, p. 1305–1340. In D. M. Knipe, P. M. Howley, D. E. Griffin, R. A. Lamb, M. A. Martin, B. Roizman, and S. E. Straus (ed.), *Fields virology*, 4th ed. Lippincott Williams & Wilkins, Philadelphia, Pa.
25. Makarova, O. V., E. M. Makarov, R. Sousa, and M. Dreyfus. 1995. Transcribing of *Escherichia coli* genes with mutant T7 RNA polymerases: stability of lacZ mRNA inversely correlates with polymerase speed. *Proc. Natl. Acad. Sci. USA* **92**:12250–12254.
26. Nanche, D., G. Varior-Krishnan, F. Cervoni, T. F. Wild, B. Rossi, C. Raibourdin-Combe, and D. Gerlier. 1993. Human membrane cofactor protein (CD46) acts as a cellular receptor for measles virus. *J. Virol.* **67**:6025–6032.
27. Ogura, H., K. Baczko, B. K. Rima, and V. ter Meulen. 1987. Selective inhibition of translation of the mRNA coding for measles virus membrane protein at elevated temperatures. *J. Virol.* **61**:472–479.
28. Portner, A., and K. G. Murti. 1986. Localization of P, NP, and M proteins on Sendai virus nucleocapsid using immunogold labeling. *Virology* **150**:469–478.
29. Qanungo, K. R., D. Shaji, M. Mathur, and A. K. Banerjee. 2004. Two RNA polymerase complexes from vesicular stomatitis virus-infected cells that carry out transcription and replication of genome RNA. *Proc. Natl. Acad. Sci. USA* **101**:5952–5957.
30. Radecke, F., P. Spielhofer, H. Schneider, K. Kaelin, M. Huber, C. Dotsch, G. Christiansen, and M. A. Billeter. 1995. Rescue of measles viruses from cloned DNA. *EMBO J.* **14**:5773–5784.
31. Rager, M., S. Vongpunsawad, W. P. Duprex, and R. Cattaneo. 2002. Polyploid measles virus with hexameric genome length. *EMBO J.* **21**:2364–2372.
32. Reutter, G. L., C. Cortese-Grogan, J. Wilson, and S. A. Moyer. 2001. Mutations in the measles virus C protein that up regulate viral RNA synthesis. *Virology* **285**:100–109.
33. Rima, B. K. 2000. Measles virus. *Nature encyclopedia of life sciences*. Nature Publishing Group., London, United Kingdom. [Online.] <http://www.els.net/doi:10.1038/npg.els.0000418>.
34. Roux, L., and F. A. Waldvogel. 1981. Establishment of Sendai virus persistent infection: biochemical analysis of the early phase of a standard plus defective interfering virus infection of BHK cells. *Virology* **112**:400–410.
35. Rubio, C., C. Kolakofsky, V. M. Hill, and D. F. Summers. 1980. Replication and assembly of VSV nucleocapsids: protein association with RNPs and the effects of cycloheximide on replication. *Virology* **105**:123–135.
36. Ryan, K. W., K. G. Murti, and A. Portner. 1990. Localization of P protein binding sites on the Sendai virus nucleocapsid. *J. Gen. Virol.* **71**:997–1000.
37. Shoji, Y., S. Inoue, K. Nakamichi, I. Kurane, T. Sakai, and K. Morimoto. 2004. Generation and characterization of P gene-deficient rabies virus. *Virology* **318**:295–305.
38. Spann, K. M., P. L. Collins, and M. N. Teng. 2003. Genetic recombination during coinfection of two mutants of human respiratory syncytial virus. *J. Virol.* **77**:11201–11211.
39. Spehner, D., R. Drillien, and P. M. Howley. 1997. The assembly of the measles virus nucleoprotein into nucleocapsid-like particles is modulated by the phosphoprotein. *Virology* **232**:260–268.
40. Thorne, H., and E. Dermott. 1976. Circular and elongated linear forms of measles virus nucleocapsid. *Nature* **264**:473–474.
41. Tober, C., M. Seufert, H. Schneider, M. A. Billeter, I. C. Johnston, S. Niewiesk, V. ter Meulen, and S. Schneider-Schaulies. 1998. Expression of measles virus V protein is associated with pathogenicity and control of viral RNA synthesis. *J. Virol.* **72**:8124–8132.
42. Udem, S. A. 1984. Measles virus: conditions for the propagation and purification of infectious virus in high yield. *J. Virol. Methods* **8**:123–136.
43. van Binnendijk, R. S., R. W. J. van der Heidjen, G. van Amerongen, and A. D. M. E. Osterhaus. 1994. Viral replication and development of specific immunity in macaques after infection with different measles virus strains. *J. Infect. Dis.* **170**:443–448.
44. Vincent, S., I. Tigaud, H. Schneider, C. J. Buchholz, Y. Yanagi, and D. Gerlier. 2002. Restriction of measles virus RNA synthesis by a mouse host cell line: trans-complementation by polymerase components or a human cellular factor(s). *J. Virol.* **76**:6121–6130.